Multiscale Modeling of Viscoelastic Properties of Polymer Nanocomposites

OLEG BORODIN,[1] DMITRY BEDROV,[1] GRANT D. SMITH,[1,2] JOHN NAIRN,[1] SCOTT BARDENHAGEN[3]

[1]Department of Materials Science and Engineering, University of Utah, Salt Lake City, Utah 84112

[2]Department of Chemical and Fuels Engineering, University of Utah, Salt Lake City, Utah 84112

[3]Group T-14, MS B214, Los Alamos National Laboratory, Los Alamos, New Mexico 87545

Received 12 August 2004; revised 6 December 2004; accepted 6 December 2004
DOI: 10.1002/polb.20390
Published online in Wiley InterScience (www.interscience.wiley.com).

ABSTRACT: A methodology for simple multiscale modeling of mechanical properties of polymer nanocomposites has been developed. This methodology consists of three steps: (1) obtaining from molecular dynamics simulations the viscoelastic properties of the bulklike polymer and approximating the position-dependent shear modulus of the interfacial polymer on the basis of the polymer-bead mean-square displacements as a function of the distance from the nanoparticle surface, (2) using bulk- and interfacial-polymer properties obtained from molecular dynamics simulations and performing stress–relaxation simulations of the nanocomposites with material-point-method simulations to extract the nanocomposite viscoelastic properties, and (3) performing direct validation of the average composite viscoelastic properties obtained from material-point-method simulations with those obtained from the molecular dynamics simulations of the nanocomposites. © 2005 Wiley Periodicals, Inc. J Polym Sci Part B: Polym Phys 43: 1005–1013, 2005
Keywords: polymer nanocomposites; molecular dynamics; material point method

INTRODUCTION

The addition of fillers is one of the avenues for altering the viscoelastic properties of polymers while maintaining the desired characteristics of a given polymer matrix, such as chemical inertness, temperature stability, electrical properties, and self-healing properties. In contrast to conventional particle–polymer composites, the addition of nanofillers with large specific interfacial areas between solid surfaces and a polymer matrix offers additional capability for the control of nanocomposite properties through the modification of the viscoelastic properties of the interfacial polymer.[1–7] Specifically, experimental studies have found that the viscoelastic properties of nanocomposite are strongly influenced not only by the nanoparticle surface fraction but also by the nanoparticle surface chemistry (modification).[8] Coarse-grained and atomistic molecular dynamics (MD) and Monte Carlo simulations[1,7,9–11] have provided valuable insight into factors responsible for the alteration of polymer matrix properties with the addition of interfaces. The main conclusion of those studies is that the strength of the nanoparticle–polymer interaction, the nanoparticle specific surface area, the surface structure, and the proximity to the glass transition are the most important factors controlling the properties of the interfacial polymer. For example, the addition of nanoparticles with attractive interactions leads to decreased polymer dynamics and increased viscosity and time-dependent shear modulus of the polymer matrix, whereas the addition of nanoparticles with repulsive, or excluded-volume, interactions leads

Correspondence to: O. Borodin (E-mail: oleg.borodin@utah.edu)

Journal of Polymer Science: Part B: Polymer Physics, Vol. 43, 1005–1013 (2005)

to increased polymer dynamics and decreased viscosity and time-dependent shear modulus. These effects scale linearly with the specific surface area of nanoparticles and increase as the temperature decreases. Another important factor controlling interfacial-polymer dynamics is the structure of the surface. A polymer next to structureless, or flat, surfaces with attractive surface–polymer interactions exhibits quite different dynamics than a polymer near structured surfaces. In the latter case, polymer motion near the surface is strongly correlated to the surface structure.

Although these studies have provided detailed recipes for altering a polymer matrix to modify nanocomposite properties, no simple methodology exists to accurately predict the viscoelastic properties of random and aggregated polymer nanocomposites containing tens and hundreds of nanoparticles. Indeed, theoretical and empirical expressions work well for regular composites, in which the majority of the polymer has bulk-polymer properties,[12–15] but they fail to predict the viscoelastic properties of nanocomposites, in which a large fraction of the polymer is situated at the nanoparticle–polymer interface and which, therefore, have properties different from those of the bulk polymer. Even when the third component (interfacial polymer) is introduced to the theoretical estimates, it is not clear how to estimate the size of the interfacial layer and its time-dependent properties and how they depend on the filler concentration.

MD simulations are well suited for predicting the viscosity and time-dependent shear modulus of polymer nanocomposites with unentangled or weakly entangled polymers, but they are limited to systems with only a few nanoparticles at best. They provide the overall mechanical properties of composites, but it is less clear how to obtain the position- and time-dependent shear modulus from MD simulations for systems with complicated geometries, which is needed as an input for the interfacial-polymer properties in theoretical models or in larger scale simulations with finite elements or similar techniques.

In this short report, we discuss a simple methodology for upscaling position-dependent polymer properties from MD simulations into continuum level modeling with the subsequent validation against MD simulations. The key supposition tested in this work is that the influence of a solid material embedded in a polymer matrix on the interfacial-polymer shear modulus is similar to its influence on the polymer-bead mean-square displacements (MSDs). This approximation allows us to infer the position-dependent shear modulus of the interfacial polymer from an analysis of the MSDs as a function of separation from the surface. The latter can be straightforwardly performed in MD simulations. The position-dependent interfacial-polymer shear modulus from such an approximation and the properties of the bulklike polymer and solid material are then used in the material-point-method (MPM) simulations of nanocomposites to obtain the average mechanical properties of the composites. Finally, a comparison of the average properties from MD and MPM simulations is made to draw conclusions about the validity of the approximations made in the calculations of the position-dependent shear modulus used in the MPM simulations.

The methodology is tested on six systems consisting of a nanocylinder embedded in a polymer matrix with three polymer volume fractions for two strengths of the polymer–surface interactions. We have chosen MPM to perform simulations on the upper scale, with the properties of all components taken from previously performed MD simulations (lower scale). In brief, MPM, which is a particle-based method,[16,17] provides a new and demonstrated method for solving equations for solid mechanics. It has significant advantages over finite element analysis (FEA) when complicated structures such as nanocomposite membranes, foams, and fabric-reinforced composites are discretized. These structures are difficult to analyze by FEA but are very easily implemented in MPM. MPM has further advantages when position-sensitive material properties, such as the transport properties of the polymer matrix, are implemented as a function of the distance from the polymer–particle interface. In MPM, each material point can be assigned different material properties, including different properties to particles within the same background grid element. Handling position-dependent material properties in FEA is much more difficult and further complicates the meshing process. In summary, MD input into full-scale MPM simulations provides a good approach to the multiscale modeling of complicated geometries with interaction-dependent mechanical and transport properties.

This article is organized as follows. In the second section, we describe in detail the methodology of the MD and MPM simulations. In the third section, we present the methodology for

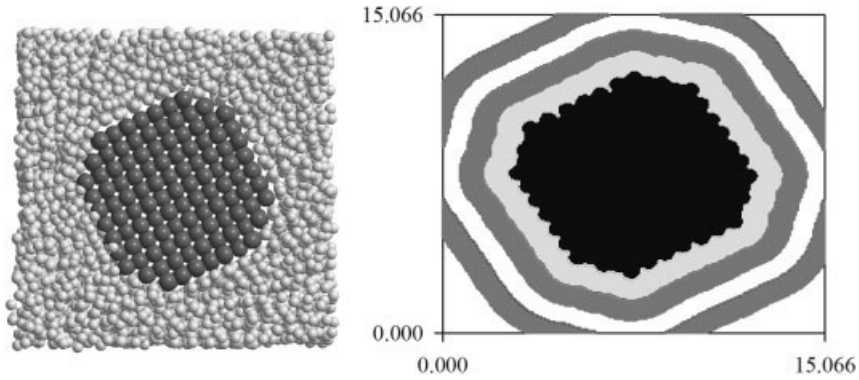

Figure 1. Snapshots of MD simulations of a cylinder embedded in a polymer matrix and an equivalent system used in MPM simulations with the filler v_f value of 30%. The material points within 0.41σ of the cylinder surface bead positions and inside the cylinder have been assigned the fcc crystal properties. Four interfacial-polymer layers and bulk polymer are shown in different colors.

approximating the time-dependent shear modulus of the interfacial polymer from MD simulations together with the MPM simulations of polymer composites with position-dependent interfacial properties. These are compared with the results of the MD simulations of the corresponding composites.

SIMULATIONS METHODOLOGIES

MD Simulations

All MD simulations were performed with the simulation package Lucretius,[18] which was modified to include the truncated and shifted Lennard–Jones potential as used in our previous work.[9] A coarse-grained representation of the polymer chains, called bead-necklace chains, used previously in our simulations of self-assembly in polymer melts and solutions, was employed in this study.[19] Each linear polymer chain consisted of 20 force centers (beads). Relatively short chains were chosen for this initial investigation to reduce the computational cost. Studies of higher molecular weight polymers will be reported later. The bond lengths were constrained to 0.935 with the Shake[20] algorithm. All polymer beads interacted according to a Lennard–Jones pair potential, $4\varepsilon_{pp}[(\sigma/r_{ij})^{12} - (\sigma/r_{ij})^{6}]$, where r_{ij} is the separation between beads i and j, that was truncated and shifted to yield zero energy and force at the truncation radius 2.5σ and $\varepsilon_{pp} = 1$. In addition to a pure polymer melt, three polymer nanocomposites consisting of a periodic cylinder embedded in a polymer matrix, as shown in Figure 1, were simulated at temperature $T^* = 0.6$ (in units of ε/k_B) in an orthorhombic periodic cell for two strengths of the cylinder surface–polymer interactions, $\varepsilon_{sp} = 1$ and $\varepsilon_{sp} = 2$. The number of polymer chains in each system, the estimated cylinder volume fractions, the simulation times, and the dimensions of the simulation box are summarized in Table 1. In this article, we refer to the nanocomposite system containing 100 polymer chains and a cylinder as the system with a cylinder nominal volume fraction, v_f, of 30%, to the nanocomposite containing 50 polymer chains and a cylinder as the $v_f = 36\%$ composite, and to the nanocomposite containing 50 polymer chains and a cylinder as the $v_f = 46\%$ composite. The cylinder had the same dimensions in all the composites. We obtained it by cutting the face-centered-cubic (fcc) lattice, as shown in Figure 1, and it had an approximate diameter of 8.4σ. The cylinder beads were included in the integration but exhibited only vibrational motion as the Lennard–Jones parameters for the interactions within the solid cylinder were set to $\varepsilon_{ss} = 5$ and $\sigma_{ss} = \sigma_{pp}$. The simulation time step was set to a typical value of $\delta t = 1.18 \times 10^{-3}$ [in units of $m\sigma^2/\varepsilon)^{1/2}$]. The mass of the polymer and cylinder bead was assumed to be 12 g/mol. Equilibration runs were performed in an NPT ensemble with stress tensor components $P_{xx} = 0$, $P_{yy} = 0$, and $P_{yy} = 0$ with the extended ensemble method of Martyna et al.[21] The average densities from the NPT runs were then used in NVT equilibration runs. We performed short MD simulations (10^5 time steps) on the polymer bulk with $\varepsilon_{pp} = 2$ after quenching the equilibrated $\varepsilon_{pp} = 1$ bulk system at $T^* = 0.6$ by increasing bead–bead interactions by a factor of two. These simulations

Table 1. Characteristics of the Bulk Polymer and Polymer Nanocomposites Investigated by MD Simulations

Polymer Chains	$\varepsilon_{s/p}^{a}$	Estimated v_f^{b}	Box Lengths x and z (σ)	Equilibration Time[c]	Production Run Length[c]
Bulk polymer					
100	N/A	0	12.67 and 12.67	5×10^4	1×10^5
Nanocomposites					
100	1	30	15.2275 and 12.4924	6×10^4	2×10^5
100	2	29	15.0657 and 12.5515	1×10^5	2×10^5
75	1	36	13.8357 and 12.491	8×10^4	3×10^5
75	2	35	13.6452 and 12.5465	2×10^5	3×10^5
50	1	46	12.266 and 12.4888	1.2×10^5	8×10^5
50	2	44	12.0800 and 12.5540	4×10^5	1×10^6

[a] In Reduced units of ε/k_B.
[b] Estimated in MD simulations as $(V_{comp}–V_{pol})/V_{comp}$, where V_{comp} is the composite volume and V_{pol} is the polymer volume estimated from bulk-polymer simulations.
[c] In reduced units of $(m\sigma^2/\varepsilon)^{1/2}$.

were used to estimate the shear modulus of a polymer glass mentioned later.

The shear transverse stress–relaxation modulus, $G_{xy}(t)$, for a polymer filled with a cylinder was calculated with the time autocorrelation function of the stress tensor:

$$G_{xy}(t) = \frac{V}{k_B T} \langle P_{xy}(t) P_{xy}(0) \rangle \qquad (1)$$

where $P_{xy}(t)$ is an instantaneous value of the off-diagonal element of the composite stress tensor at time t in the plane (xy) perpendicular to direction of the cylinder located along the z direction, V is the volume of the system, and the brackets denote the averaging over the whole trajectory. The bulk shear modulus of the polymer was obtained by the averaging of three off-diagonal elements of the symmetric stress tensor.

MD simulations of the bulk fcc crystal consisting of 2048 beads were performed for at least 10^5 time steps, $\delta t = 11.8 \times 10^{-4}$ [in units $(m\sigma^2/\varepsilon)^{1/2}$], at 0 and 0.1% strain to estimate the crystal elastic constants needed for MPM simulations of composites. The isotropic approximations of the shear modulus, G, and bulk modulus, K, for the Lennard–Jones crystal were obtained with a Reuss average.[22] The resulting values of the crystal were $G = 130$ and $K = 270$ (in reduced units).

MPM

A number of MPM stress–relaxation experiments were performed to extract the average stress response to the application of the almost instantaneous stress applied for composites corresponding to those used in the MD simulations and summarized in Table 1. Two-dimensional NairnMPM code[23] was used. An accurate representation of the position-dependent viscoelastic properties of the interfacial polymer was ensured with a significant number of material points, 200 × 200 (4 per element). The time-dependent polymer shear modulus, $G(t)$, of the bulk and interfacial polymer was represented with a sum of four or five exponents. The usage of a sum of exponentials allows faster calculation of the viscoelastic response than the usage of a stretched exponential because only material properties from the previous time step have to be stored for each exponent; this is more efficient than storing and integrating material properties for all points for all times as required for the stretched exponentials often used in the description of $G(t)$ in MD simulations.

A computational stress–relaxation experiment was performed in the following way. At time $t = 0$, all materials were stress- and strain-free. We applied strain for all material points adjacent to the $x = 0$ boundary along the y axis to the system by linearly increasing velocity $v_y = 0.001\, t$ ($x = 0$) for time t_0, then keeping the velocity constant for the same interval t_0, and finally linearly scaling velocity to zero over the time interval $[2t_0{:}3t_0]$, where t_0 is 10^{-3}. The other boundary condition was $v_y(x = L) = 0$, where L is the linear dimension of the system. The default (for MPM) no-slip condition was used. The particle stress

state was updated twice, before the particle position was updated and after the particle position was updated, as it was found to lead to better energy conservation.[16] K of the polymer was assumed to be time- and position-independent and was obtained from linear fit to the pressure–volume dependence of the bulk polymer calculated from short MD simulations ($t = 200$).

MD: MPM LINKAGE

To predict the overall nanocomposite (see Fig. 1) viscoelastic properties in MPM simulations, we need to specify position-dependent $G(t)$ for the polymer and elastic modulus for the cylinder. When the interfacial-polymer fraction is negligible or the solid interface does not perturb polymer relaxation, both bulk-polymer and bulk-cylinder properties can be obtained from MD simulations or experiments. Difficulties arise, however, when the filler significantly changes the interfacial-polymer viscoelastic properties and the fraction of the interfacial polymer becomes significant, as is frequently observed for nanocomposites. The calculation of position-dependent $G(t)$ is a complicated problem, and we would like to avoid it by approximating position-dependent $G(t)$ with more easily accessible properties. A polymer-bead MSD is a dynamic process that is expected to be closely related to a momentum transfer in polymers quantified by $G(t)$. Position-dependent bead displacements along the surface are also readily accessible from MD simulations. Here, we assume that position-dependent $G^{\text{layer } i}(t)$, that is, the shear modulus for each interfacial layer, in polymer nanocomposites can be approximated by the scaling of its time axis on the basis of the behavior of polymer-bead displacements along the interface:

$$G^{\text{layer } i}(t) = G_{\text{bulk}}\left[t^* a^{\text{layer } i}(t)\right] \qquad (2)$$

where $G_{\text{bulk}}[t^*]$ is bulk polymer shear modulus. The shift factor $a^{\text{layer } i}(t)$ is determined for each layer as follows:

$$\text{MSD}^{\text{layer } i}\left[t/a^{\text{layer } i}(t)\right] = \text{MSD}_{\text{bulk}}(t) \qquad (3)$$

where $\text{MSD}^{\text{layer } i}$ is the polymer-bead mean-square displacement of beads in interfacial layer i and $\text{MSD}_{\text{bulk}}(t)$ is the polymer-bead mean-square displacement of beads in the bulk polymer calculated for a slab of the same thickness as layer i.

This approximation is based on two assumptions: (1) the position-dependent shear modulus is isotropic and (2) an increase in the polymer-bead dynamics by a time-dependent shift factor, $a(t)$, leads to a corresponding decrease in the decay of the relaxation time $G(t)$ by the same factor $a(t)$. The first assumption could only be indirectly supported by observations that polymer-bead diffusion near nanoparticles in the radial direction was approximately equal to that perpendicular to a nanoparticle.[11] The second assumption is usually accurate for polymer melts and also inherent in a widely used Rouse model. Furthermore, we have assumed that the position-dependent properties are dependent only on the shortest distance from the nanoparticles and the distance between nanoparticles through periodic boundary conditions.

Similarly to our previous analysis of a polymer sandwiched between two surfaces,[9] in which we divided the interfacial polymer into layers with peaks in the density profile, we calculated the polymer density versus the distance to the closest surface bead, as shown in Figure 2, and used these density profiles to divide the interfacial polymer into layers. The first peak is well pronounced for both $\varepsilon_{\text{sp}} = 1$ and especially $\varepsilon_{\text{sp}} = 2$ composites and indicates a significant correlation between the interfacial polymer and surface structure. The second peak is much less pronounced but is clearly identifiable for all the composites. The positions of the first two peaks are similar for all the composites, whereas their magnitude increases slightly with decreasing polymer content; this indicates the presence of the polymer confinement effect between one surface of the cylinder and a periodic image on the other side of the cylinder. The third peak is less distinct than the second one; moreover, its position depends on the concentration of the filler, and this further indicates polymer confinement effects. To consistently analyze interfacial-polymer dynamics in all the composites, we defined the first and second layers by the corresponding minima in the density profiles, whereas the width of the third and forth layers were set to 0.9σ for all the composites.

The polymer-bead MSDs for the first three layers were calculated and are shown in Figure 3 for all the composites. As expected, the composites with the attractive surface–polymer inter-

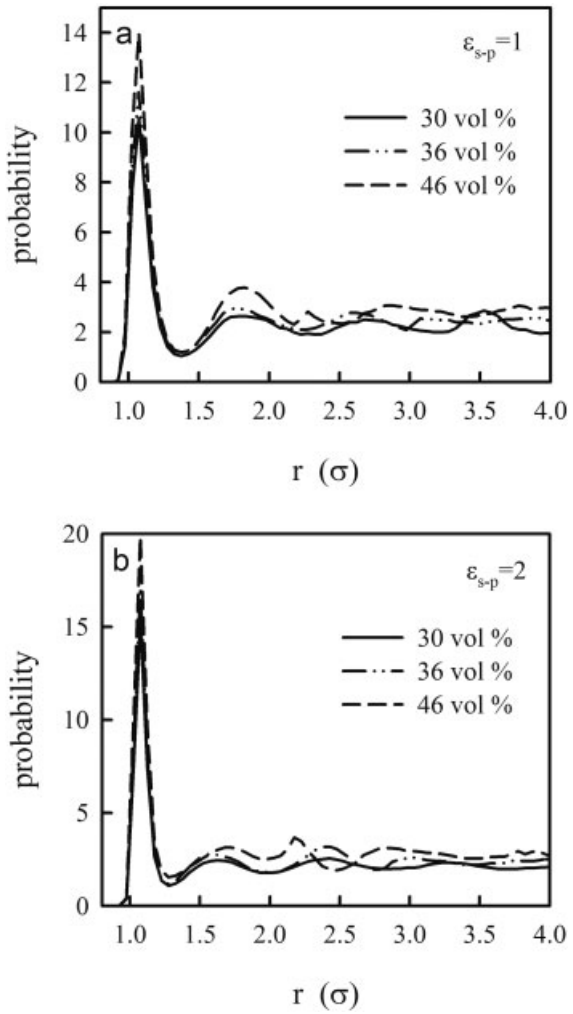

Figure 2. Polymer density profile (in arbitrary units) versus the distance to the closest surface bead for composites with the polymer–surface interactions (a) $\varepsilon_{sp} = 1$ and (b) $\varepsilon_{sp} = 2$.

actions $\varepsilon_{sp} = 2$ exhibited interfacial-polymer (layers 1 and 2) MSDs multiple orders of magnitude slower than those of the composites with the neutral surface–polymer interaction $\varepsilon_{sp} = 1$. Nevertheless, the slowdown of the interfacial polymer for the $\varepsilon_{sp} = 1$ composites is significant (e.g., about a factor of 10 for the first interfacial layer and a factor of 3 for the second layer) and, therefore, needs to be included in MPM calculations for the neutral composite to obtain accurate average properties, as shown later. Another feature clearly shown in Figure 3 is the interfacial-polymer slowdown with a decreasing polymer volume fraction for the composites. This can be attributed to the confinement of the polymer between the cylinder surfaces.

In the next step, we calculated $a(t)$ (see eqs 2 and 3) for each polymer layer for all the composites and substituted them in the approximation by $G_{\text{bulk}}[t^*a^{\text{layer } i}(t)]$. The resulting $G^{\text{layer } i}(t)$ values for the $v_f = 30\%$ composite are shown in Figure 4. For very short times ($t < 0.2$), all the $G(t)$ curves superimpose on one another because for such short times bead MSDs are the same. This indicates that the bead ballistic motion regime is not significantly affected by the presence of solid interfaces. Interestingly, $G(t)$ for layer 1 of the $\varepsilon_{sp} = 2$ composite is very similar to the bulk-polymer $G(t)$ for the $\varepsilon_{pp} = 2$ melt (not shown in Fig. 4).

In the next step, MPM stress–relaxation computational experiments were performed for composites with the $\varepsilon_{sp} = 1$ and $\varepsilon_{sp} = 2$ surface–polymer interactions to obtain average composite

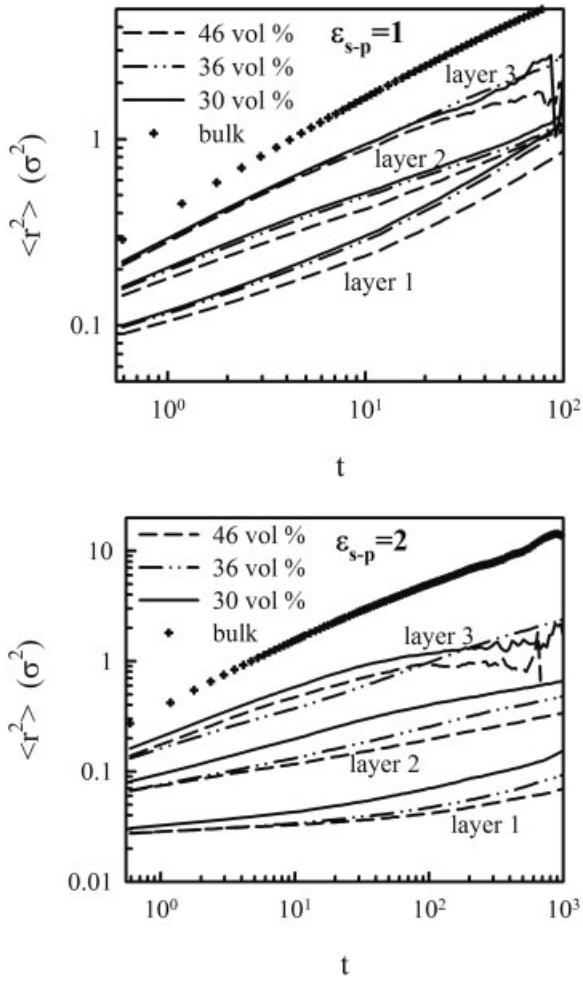

Figure 3. MSDs of the interfacial-polymer beads $\langle r^2 \rangle$ for the $\varepsilon_{sp} = 1$ and $\varepsilon_{sp} = 2$ composites with cylinder v_f values of 30, 36, and 46% and for the bulk polymer.

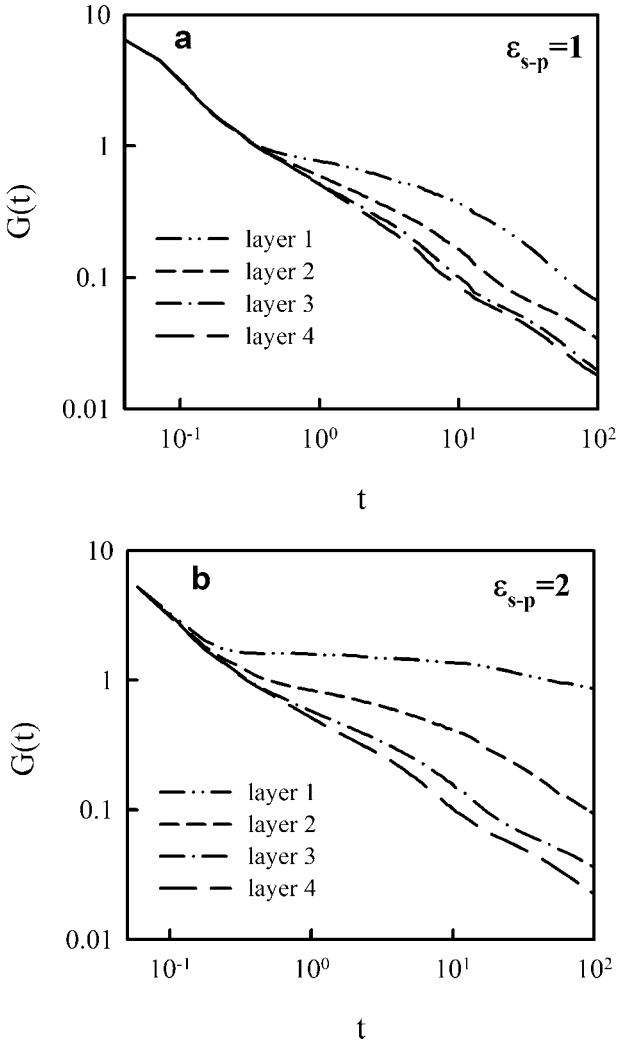

Figure 4. Time-dependent $G(t)$ for the interfacial polymer for composites with the cylinder v_f value of 30% and the surface–polymer interactions (a) $\varepsilon_{sp} = 1$ and (b) $\varepsilon_{sp} = 2$.

mechanical properties. MPM simulations were also performed for a cylinder embedded in a polymer that had bulk-polymer properties corresponding to the case of no influence of the solid cylinder on the interfacial-polymer properties. A layout of the material points in the MPM simulations of the composites is shown in Figures 1 and 5. The average time-dependent shear moduli from the MD and MPM simulations for the pure polymer melt and for transverse component $G(t)$ of the polymer nanocomposites are shown in Figure 6. For all concentrations, as expected, the two-material (bulklike polymer and elastic cylinder) model predicted a lower composite shear modulus because it ignored the interfacial-polymer slowdown. The inclusion of the interfacial polymer led to a slightly higher $G(t)$ for the cylinder $v_f = 30\%$ composite for both $\varepsilon_{sp} = 1$ and $\varepsilon_{sp} = 2$ surface–polymer interactions. For the $v_f = 36\%$ composite, excellent agreement was observed between the MPM predictions that included interfacial effects and the MD simulation results. Finally, for the $v_f = 46\%$ composite, excellent agreement between the MD and MPM simulations was found for $\varepsilon_{sp} = 1$, whereas for the $\varepsilon_{sp} = 2$ composite, the MPM simulations predicted somewhat lower $G(t)$ values than the MD results. Nevertheless, even for this system, most of the increase in the shear modulus due to surface–polymer interactions was adequately captured in the MPM simulations.

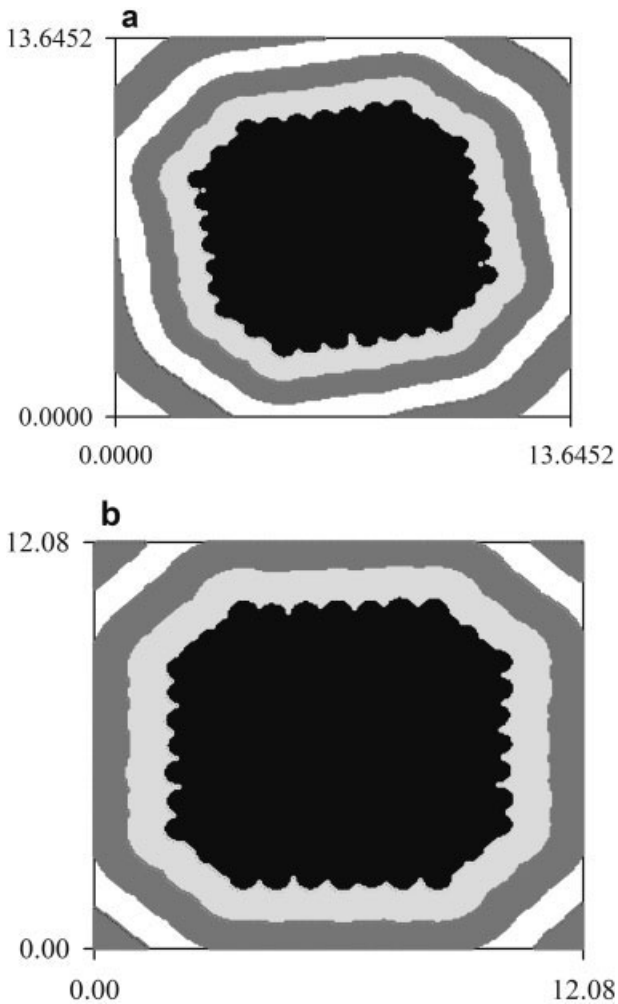

Figure 5. Layout of material points representing a cylinder. The different colors indicate four interfacial-polymer layers and a bulklike polymer in polymer nanocomposites with cylinder v_f values of 36 and 46% used in the MPM simulations. The cylinder position was taken from the final snapshot of the MD simulations. It did not change significantly over the production run.

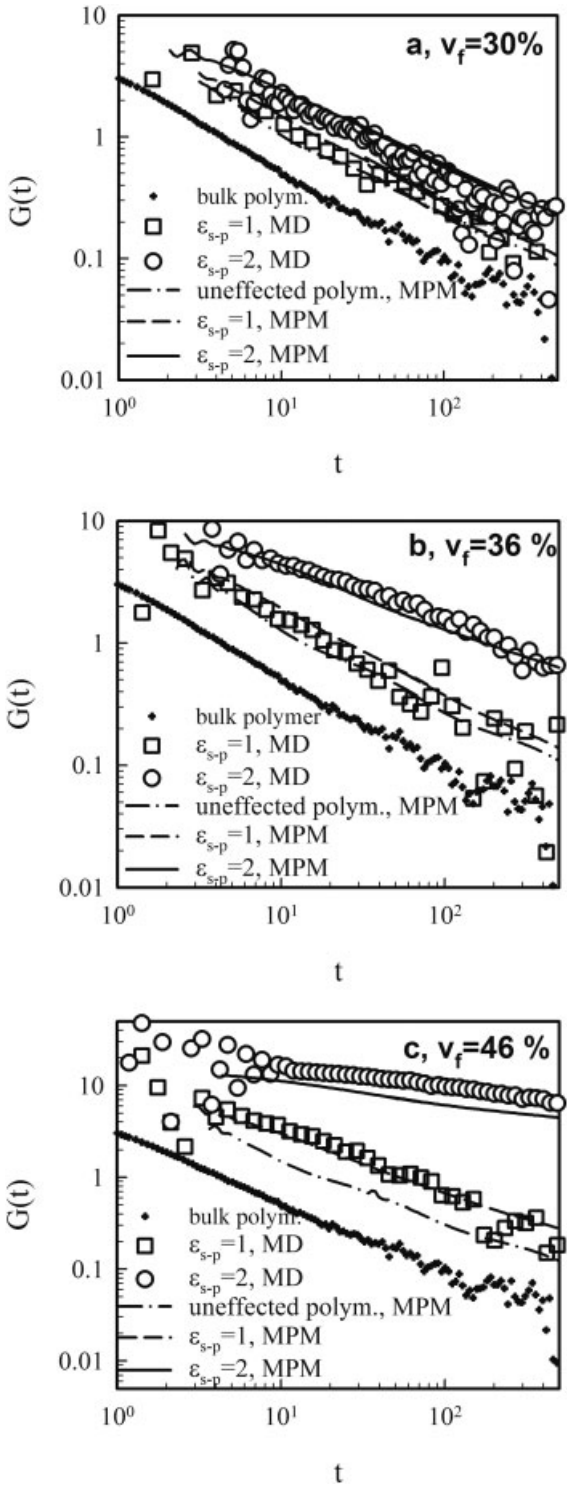

Figure 6. Time-dependent $G(t)$ of the bulk polymer and periodic composites with the $\varepsilon_{sp} = 1$ and $\varepsilon_{sp} = 2$ surface–polymer interactions from the MD and MPM simulations. The results of the MPM simulations of the composites consisting of the bulklike (unaffected) polymer and elastic cylinder at geometries corresponding to those of the $\varepsilon_{sp} = 1$ composites are also shown.

CONCLUSIONS

A simple methodology for including the interfacial-polymer time-dependent shear modulus in MPM calculations was developed and validated for nanocomposites consisting of a cylinder embedded in a polymer matrix. The key approximation, that the influence of a solid material embedded in a polymer matrix on the interfacial-polymer shear modulus is similar to its influence on the polymer-bead MSDs, allowed us to determine the position-dependent shear modulus of the interfacial polymer from the analysis of the MSDs as a function of separation from the surface. The validity of this approximation was confirmed by a comparison of the composite mechanical properties from MPM simulations, for which the aforementioned assumption was used to determine the interfacial-polymer shear modulus, with the results of MD simulations that did not require any assumptions for determining the overall composite shear modulus.

MPM and MD simulations of periodic nanocomposites with attractive interfaces indicated that turning on attraction between the polymer and cylinders could increase the time-dependent shear modulus by multiple orders of magnitude, with the increase being more substantial at longer times.

The authors gratefully acknowledge the support of the U.S. Department of Energy through grant DEFG0301ER45914 and support through the University of Utah Center for the Simulation of Accidental Fires and Explosions (C-SAFE), funded by Department of Energy, Lawrence Livermore National Laboratory, under Subcontract B341493.

REFERENCES AND NOTES

1. Monte Carlo and Molecular Dynamics Simulations in Polymer Science; Binder, K., Ed.; Oxford University Press: New York, 1995.
2. Krishnamoorti, R.; Ren, J.; Silva, A. S. J Chem Phys 2001, 114, 4968.
3. Cole, D. H.; Shull, K. R.; Baldo, R.; Rehn, L. Macromolecules 1999, 32, 771.
4. Tsagaropoulos, G.; Eisenberg, A. Macromolecules 1995, 28, 396.
5. Tsagaropoulos, G.; Eisenberg, A. Macromolecules 1995, 28, 6067.
6. van Zanten, J. H.; Wallace, W. E.; Wu, W. L. Phys Rev E 1996, 53, 2053.
7. Starr, F. W.; Schrøder, T. B.; Glotzer, S. Phys Rev E 2001, 64, 021802.

8. Zhang, Q.; Archer, L. A. Langmuir 2002, 18, 10435.
9. Smith, G. D.; Bedrov, D.; Borodin, O. Phys Rev Lett 2003, 90, 226103.
10. Borodin, O.; Smith, G. D.; Bandyopadhyaya, R.; Buytner, O. Macromolecules 2003, 36, 7873.
11. Starr, F. W.; Douglas, J. D.; Glotzer, S. C. J Chem Phys 2003, 119, 1777.
12. Hashin, Z. J Appl Mech 1983, 50, 481.
13. Torquato, S. Appl Mech Rev 1991, 44, 37.
14. Milton, G. W. Phys Rev Lett 1981, 46, 542.
15. Buryachenko, V. A. Appl Mech Rev 2001, 54, 1.
16. Nairn, J. A. Comput Model Eng Sci 2003, 4, 649.
17. Sulsky, D.; Zhou, S.-J.; Schreyer, H. L. Comput Phys Commun 1995, 87, 236.
18. Lucretius: A Molecular Simulation Package. http://www.che.utah.edu/~gdsmith/mdcode/main.html.
19. Mendez, S.; Curro, J. G.; Pütz, M.; Bedrov, D.; Smith, G. D. J Chem Phys 2001, 115, 5669.
20. Palmer, B. J. J Comput Phys 1993, 104, 470.
21. Martyna, G. J.; Tuckerman, M.; Tobias, D. J.; Klein, M. L. Mol Phys 1996, 87, 1117.
22. Sewell, T. D.; Menikoff, R.; Bedrov, D.; Smith, G. D. J Chem Phys 2003, 119, 7417.
23. The NairnMPM simulation package is available for free at http://nairn.mse.utah.edu.